

## Optical band gap and luminescence study of yttrium doped neodymium lead borotellurite glass system

S. N. M. Rafien<sup>a</sup>, A. Hashim<sup>b,\*</sup>, H. Laoding<sup>c</sup>, W. A. W. Razali<sup>c</sup>, N. Yahya<sup>c</sup>

<sup>a</sup>*Faculty of Applied Sciences, Universiti Teknologi MARA, 40450 Shah Alam, Selangor, Malaysia*

<sup>b</sup>*Faculty of Plantation and Agrotechnology, Universiti Teknologi MARA Cawangan Melaka, Jasin Campus, 77300 Merlimau Melaka, Malaysia*

<sup>c</sup>*Faculty of Applied Sciences, Universiti Teknologi MARA Pahang, 26400 Bandar Tun Abdul Razak Jengka, Pahang, Malaysia*

Glasses of composition  $(49-x)\text{H}_3\text{BO}_3\text{-}35\text{TeO}_2\text{-}15\text{PbO}\text{-}1.0\text{Nd}_2\text{O}_3\text{-}x\text{Y}_2\text{O}_3$  ( $x = 0.0, 0.5, 1.0, 1.5, 2.0$  and  $2.5$  mol%) were successfully prepared by a melt-quench method. The effect of  $\text{Y}_2\text{O}_3$  on the optical properties of the glasses were investigated by using Uv-Vis NIR and photoluminescence spectroscopy. X-ray diffraction pattern of the prepared glasses exhibits amorphous nature. Absorption spectra of the glasses are recorded in the range 400 – 1100 nm and shows eleven absorption peaks. In order to determine the optical band gap of the glass sample, the Uv-Vis NIR measurement has been carried out in the room temperature. The values of direct and indirect optical band gap initially decreasing before increasing, which were attributed to structural changes induced by the inclusion of  $\text{Y}_2\text{O}_3$ . The luminescence spectra were obtained under 581 nm wavelength.

(Received March 31, 2022; Accepted July 8, 2022)

*Keywords:* Yttrium, Lead, Borotellurite, Glass, Optical properties

### 1. Introduction

Glasses have distinctive properties as compared to other matters such as ceramic or metal. It is hard in strength and hardness but transparent at room temperature. Other than that, glasses have excellent resistance to corrosiveness [1]. Nowadays, glasses are increasingly used as host material for solid state laser based on rare earth ions. Since the quantum efficiency of the emission transitions depends on the structural modification of the host material, it is important to select the right host material [2]. Glasses combining borate and tellurite exhibit very interesting characteristics such as high thermal durability, high mechanical strength, low hygroscopic nature, and low phonon energy [3]. The combination of lead oxide and borotellurite glass tend to enhance the glass properties. Based on previous research done by Othman et al., (2019), when lead oxide is added into borate glass, the crystallization of the glass was proven to be prevented [4].

Meanwhile, according to Kesavulu & Jayasankar (2012), the inclusion of lead oxide into tellurite glass reduces non-radiative losses and decreases the phonon energy of the glass system [5]. Considering these advantages, lead borotellurite glasses have been chosen as a suitable host material and prove to be valuable for photonic and computing application. Among rare earth ions, neodymium ions reported by previous researchers have shown an interesting property and is also one of the excellent candidates for photonic devices [6]. Glasses based on transition metal ions (TMI) like yttrium oxide have gained great attention due to their favorable features such as higher optical, chemical, electrical, and mechanical properties [7]. Consequently, these glasses are significant in various applications such as electro-optic, electronic and electrochemical devices due to the existence of more than one valence state. The objective of this study is to analyze the influence of yttrium oxide on the optical properties of the neodymium doped lead borotellurite glass.

---

\* Corresponding author: dazhan@uitm.edu.my

<https://doi.org/10.15251/CL.2022.197.463>

## 2. Procedure

Good optical quality of glasses with the composition  $(49-x)\text{H}_3\text{BO}_3\text{-}35\text{TeO}_2\text{-}15\text{PbO}\text{-}1.0\text{Nd}_2\text{O}_3\text{-}x\text{Y}_2\text{O}_3$  ( $x = 0.0, 0.5, 1.0, 1.5, 2.0$  and  $2.5$  mol%) were prepared using melt-quenching technique with the composition as tabulated in Table 1. Batches of 15 g have been prepared by mixing high purity analytical reagent grade chemical from Sigma Aldrich (Germany), Riedel-De Haen (Germany), (United Kingdom) and Acros Organic (Belgium) with 99.9% purity for  $\text{Nd}_2\text{O}_3$ ,  $\text{Y}_2\text{O}_3$  (99.99% purity),  $\text{PbO}$  (99.0% purity),  $\text{H}_3\text{BO}_3$  (99.8% purity) and  $\text{TeO}_2$  (99% purity). The mixture produced were then melted in electrical box furnace for 30 minutes at a temperature  $1000^\circ\text{C}$ . The casting process will be carried out by pouring the molten into a pre-heated stainless-steel plate, followed by a 5-hour annealing process at a temperature  $400^\circ\text{C}$ . After that, the samples were allowed to cool down to room temperature gradually. Finally, the samples were polished using sandpaper before being used for any optical characterizations. Excessive samples were grounded into powder form for X-ray diffraction (XRD) testing.

Table 1. Nominal Composition of  $(49-x)\text{H}_3\text{BO}_3\text{-}35\text{TeO}_2\text{-}15\text{PbO}\text{-}1.0\text{Nd}_2\text{O}_3\text{-}x\text{Y}_2\text{O}_3$  Glass System.

Y <sub>2</sub> O <sub>3</sub> Concentration (mol%)	Nominal Composition (mol %)				
	Y <sub>2</sub> O <sub>3</sub>	H <sub>3</sub> BO <sub>3</sub>	TeO <sub>2</sub>	PbO	Nd <sub>2</sub> O <sub>3</sub>
0.0	0.0	49.0	35.0	15.0	1.0
0.5	0.5	48.5	35.0	15.0	1.0
1.0	1.0	48.0	35.0	15.0	1.0
1.5	1.5	47.5	35.0	15.0	1.0
2.0	2.0	47.0	35.0	15.0	1.0
2.5	2.5	46.5	35.0	15.0	1.0

## 3. Characterizations

The X-ray diffraction (XRD) analyses was carried out through X'Pert PRO/PANalytical Diffractometer. Meanwhile, the Uv-1800 spectrophotometer was used in the range of 400 nm - 1100 nm to determine the absorption spectra of the glass samples. The absorption coefficient,  $\alpha(\omega)$ , is measured by using the absorption data as following equation [8]

$$\alpha(\omega) = 2.303 \frac{A}{d} \quad (1)$$

where the absorption represented as  $A$  and the sample thickness represented as  $d$ . The optical band gap ( $E_{opt}$ ) of the prepared glasses can be evaluated based on Mott-Davis relation through direct and indirect transitions as follows [9]:

$$\alpha(\omega) = \frac{B(\hbar\omega - E_{opt})^r}{\hbar\omega} \quad (2)$$

where  $B$  is the band tailing parameter (constant),  $\hbar\omega$  is the photon energy,  $E_{opt}$  is the optical band gap energy while the value of  $r$  is dependent on the nature of interband electronic transition causing the absorption ( $r = \frac{1}{2}$  for direct transition) and ( $r = 2$  for indirect transition). Based on this relation, the graph of  $(\alpha\hbar\omega)^{1/2}$  and  $(\alpha\hbar\omega)^2$  vs  $\hbar\omega$  can be plotted and the value of optical band gap is the extrapolation of the linear region of the curves in these two graphs. In order to investigate the emission and excitation spectra of the glass samples, luminescence spectra were recorded using Pelkin Elmer Luminescence Spectrometer model LS55 with a resolution 0.1 nm in the NIR region 850 nm to 1100 nm by monitoring an excitation wavelength at 581 nm. All the measurement were conducted at room temperature.

#### 4. Results and discussions

The X-ray diffraction pattern of the glasses with the composition  $(49-x)\text{H}_3\text{BO}_3\text{-}35\text{TeO}_2\text{-}15\text{PbO}\text{-}1.0\text{Nd}_2\text{O}_3\text{-}x\text{Y}_2\text{O}_3$  ( $x = 0.0, 0.5, 1.0, 1.5, 2.0$  and  $2.5$  mol%) were recorded in the range of  $10^\circ \leq \theta \leq 90^\circ$  and are shown in Figure 1. From this figure, it can be noticed that there is no discrete lines which indicates the typical long range structural disorder and the absence of sharp peak confirmed the amorphous nature of the samples [10,11].

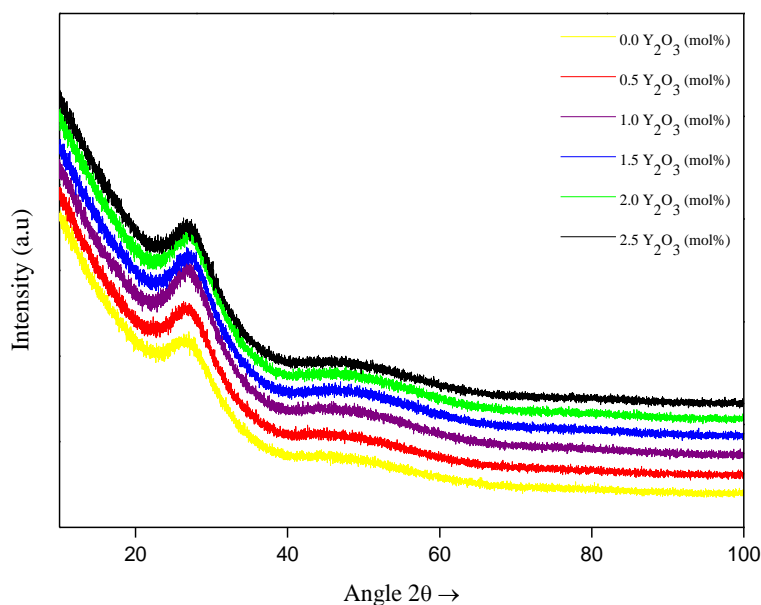


Fig. 1. XRD Spectra of  $(49-x)\text{H}_3\text{BO}_3\text{-}35\text{TeO}_2\text{-}15\text{PbO}\text{-}1.0\text{Nd}_2\text{O}_3\text{-}x\text{Y}_2\text{O}_3$  glasses.

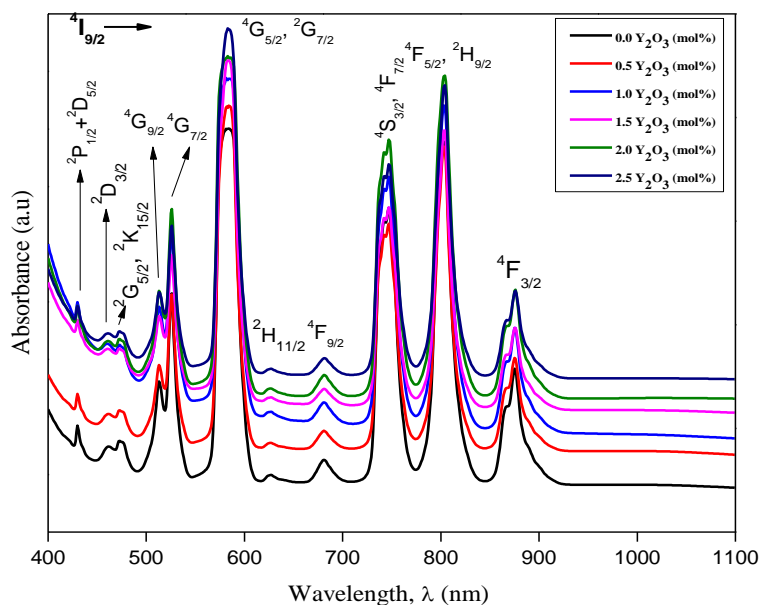


Fig. 2. Absorption spectra of  $(49-x)\text{H}_3\text{BO}_3\text{-}35\text{TeO}_2\text{-}15\text{PbO}\text{-}1.0\text{Nd}_2\text{O}_3\text{-}x\text{Y}_2\text{O}_3$  glasses

The UV-Vis NIR absorption spectra of the glass samples were presented in Figure 2. The optical absorption spectra give information regarding to the band positions and energy band gap of the amorphous material and its induced transitions. All the absorption bands are well resolved in

the ultraviolet and visible regions due to transitions of electrons from valence band to conduction bands that occur inside the glass samples. Furthermore, the absorption bands only appear due to the presence of rare earth ions in the glass system [12]. From Figure 2, the spectrum shows eleven absorption bands which attributed to the transition related to  $\text{Nd}^{3+}$  ions levels. The absorption bands correspond to the transitions from the  $^4\text{I}_{9/2}$  ground state to the  $(^2\text{P}_{1/2} + ^2\text{D}_{5/2})$ ,  $^2\text{D}_{3/2}$ ,  $(^2\text{G}_{5/2}, ^2\text{K}_{15/2})$ ,  $^4\text{G}_{9/2}$ ,  $^4\text{G}_{7/2}$ ,  $(^4\text{G}_{5/2}, ^2\text{G}_{7/2})$ ,  $^2\text{H}_{11/2}$ ,  $^4\text{F}_{9/2}$ ,  $(^4\text{S}_{3/2}, 4\text{F}_{7/2})$ ,  $(^4\text{F}_{5/2}, ^2\text{H}_{9/2})$  and  $^4\text{F}_{3/2}$  excited state, respectively. Among all the transitions, the absorption band around 581 nm which corresponding to the  $^4\text{I}_{9/2} \rightarrow ^4\text{G}_{5/2}, ^2\text{G}_{7/2}$  transition exhibits higher intensity, and this band is highly affected by  $\text{Y}^{3+}$  ions. In order to measure the emission spectra of rare earth ions, the excitation wavelength plays an important role. Therefore, an intense visible excitation band at 581 nm wavelength has been selected for the measurement of emission spectrum.

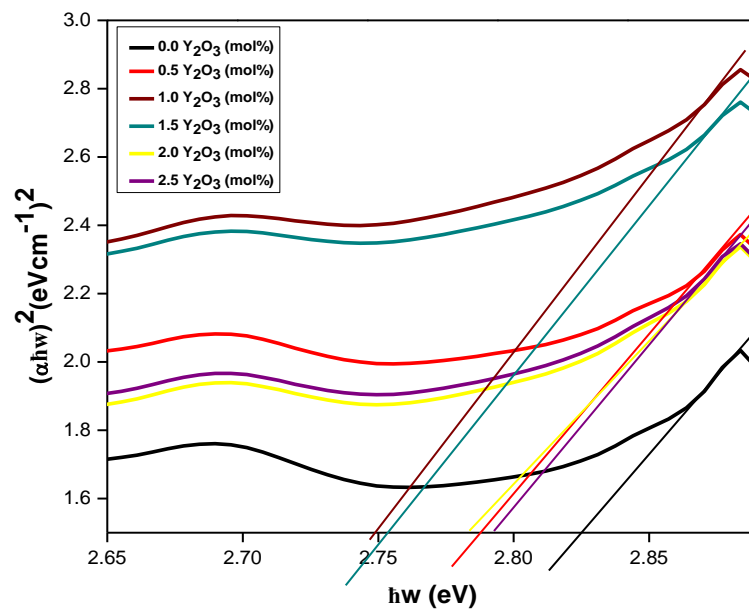


Fig. 3. Plot of  $(\alpha\hbar\omega)^2$  vs  $\hbar\omega$  for  $(49-x)\text{H}_3\text{BO}_3\text{-}35\text{TeO}_2\text{-}15\text{PbO}\text{-}1.0\text{Nd}_2\text{O}_3\text{-}x\text{Y}_2\text{O}_3$  glasses.

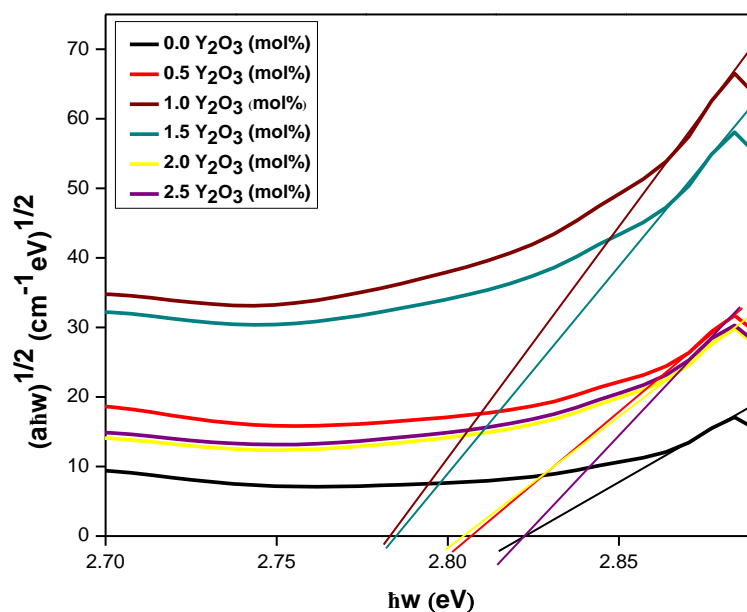


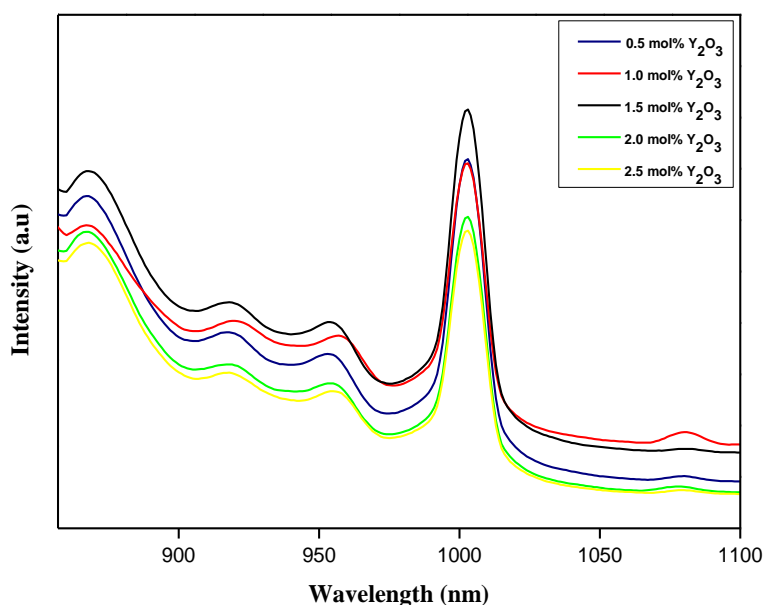
Fig. 4. Plot of  $(\alpha\hbar\omega)^{1/2}$  vs  $\hbar\omega$  for  $(49-x)\text{H}_3\text{BO}_3\text{-}35\text{TeO}_2\text{-}15\text{PbO}\text{-}1.0\text{Nd}_2\text{O}_3\text{-}x\text{Y}_2\text{O}_3$  glasses.

Table 2. Direct and indirect band gap of  $(49-x)\text{H}_3\text{BO}_3\text{-}35\text{TeO}_2\text{-}15\text{PbO}\text{-}1.0\text{Nd}_2\text{O}_3\text{-}x\text{Y}_2\text{O}_3$  glasses.

$\text{Y}_2\text{O}_3$ Concentration (mol%)	Direct $E_{opt}$ (eV)	Indirect $E_{opt}$ (eV)
0.0	2.800	2.827
0.5	2.790	2.808
1.0	2.760	2.787
1.5	2.794	2.805
2.0	2.812	2.811
2.5	2.814	2.815

Figures 3 and 4 present the graph of direct and indirect  $E_{opt}$  of the  $(49-x)\text{H}_3\text{BO}_3\text{-}35\text{TeO}_2\text{-}15\text{PbO}\text{-}1.0\text{Nd}_2\text{O}_3\text{-}x\text{Y}_2\text{O}_3$  glasses. The values of direct and indirect  $E_{opt}$  of the prepared glasses were listed in Table 2. As observed, the direct and indirect  $E_{opt}$  for the glass samples initially decreasing before increasing as the  $\text{Y}_2\text{O}_3$  concentration increasing from 0.0 mol% up to 2.5 mol%. It is interesting to note that the replacement of  $\text{H}_3\text{BO}_3$  content with  $\text{Y}_2\text{O}_3$  content in the glass system exhibits structural variation in the glass. According to Yasser *et al.*, (2016), the decrease in the values of  $E_{opt}$  might be due to some structural changes and also due to the increase of randomness of the glass network which correlated to the role of  $\text{Y}_2\text{O}_3$  as network former [13]. However, further increase in the concentration of  $\text{Y}_2\text{O}_3$  in the glass network led to the formation of more bridging oxygens which resulted in increasing the  $E_{opt}$  [14].

The emission spectra of the  $(49-x)\text{H}_3\text{BO}_3\text{-}35\text{TeO}_2\text{-}15\text{PbO}\text{-}1.0\text{Nd}_2\text{O}_3\text{-}x\text{Y}_2\text{O}_3$  glasses was presented under 581 nm excitation wavelength, as illustrated in Figure 5. All the glass samples show a broad emission peak in the NIR region of 850 nm - 1100 nm which contributed from  $\text{Nd}^{3+}$  ions. From Figure 5, it is found that the most intense emission peaks appear at 1003 nm attributed to the  ${}^4\text{F}_{3/2}$  to  ${}^4\text{I}_{13/2}$  transition. These results are consistent with the previous study by Sukul *et al.*, (2017), which studied the photoluminescence of Nd doped  $\text{Y}_2\text{O}_3$  ceramics phosphor with the optimum emission peaks at 1064 nm [15]. The emission intensity of the glass samples increases as the  $\text{Y}_2\text{O}_3$  content increase from 0 mol% up to 1.5 mol%. However, with further addition of  $\text{Y}_2\text{O}_3$  up to 2.0 mol%, the emission intensity does not increase more and sharply drops when the  $\text{Y}_2\text{O}_3$  content reach to 2.5 mol%. Decrease in the emission intensity might be attribute to the concentration quenching effect occurs due to the  $\text{Nd}^{3+}$  ions cluster in the glass system [16].

Fig. 5. Photoluminescence of  $(49-x)\text{H}_3\text{BO}_3\text{-}35\text{TeO}_2\text{-}15\text{PbO}\text{-}1.0\text{Nd}_2\text{O}_3\text{-}x\text{Y}_2\text{O}_3$  glasses

## 5. Conclusion

A series of glass with the composition of  $(49-x)\text{H}_3\text{BO}_3\text{-}35\text{TeO}_2\text{-}15\text{PbO}\text{-}1.0\text{Nd}_2\text{O}_3\text{-}x\text{Y}_2\text{O}_3$  ( $x = 0.0, 0.5, 1.0, 1.5, 2.0$  and  $2.5$  mol%) were successfully prepared and analysed using XRD, UV-Vis NIR and photoluminescence spectroscopy. The amorphous nature of the glass samples was confirmed by XRD analysis. The optimum emission intensity was observed for the sample having 1.5 mol%  $\text{Y}_2\text{O}_3$  content. Using 518 nm excitation wavelength, the highest emission peaks was obtained at 1003 nm which correspond to the  ${}^4\text{F}_{3/2}$  to  ${}^4\text{I}_{13/2}$  lasing transition.

## Acknowledgments

The authors would like to acknowledge the Ministry of Higher Education (MOHE), Malaysia for the financial support via Fundamental Research Grant Scheme (FRGS) no. 600-IRMI/FRGS 5/3 (266/2019). We acknowledge Universiti Teknologi MARA and Universiti Teknologi Malaysia for their research facilities.

## References

- [1] M. Hasanuzzaman, A. Rafferty, M. Sajjia, A.-G. Olabi, Properties of Glass Materials, Ref. Modul. Mater. Sci. Mater. Eng., October, 1-12 (2016); <https://doi.org/10.1016/B978-0-12-803581-8.03998-9>
- [2] Saba Farhan. H, Aust. J. Basic Appl. Sci., 11(9), 171-178 (2017); <https://doi.org/10.1107/S010876738708200X>
- [3] A. Madhu, B. Eraiah, P. Manasa, N. Srinatha, Opt. Mater. (Amst)., 75, 357-366 (2018); <https://doi.org/10.1016/j.optmat.2017.10.037>
- [4] H. A. Othman, A. Herrmann, D. Möncke, Int. J. Appl. Glas. Sci., 10(3), 339-348 (2019); <https://doi.org/10.1111/ijag.13100>
- [5] C. R. Kesavulu, C. K. Jayasankar, J. Lumin., 132(10), 2802-2809 (2012); <https://doi.org/10.1016/j.jlumin.2012.05.031>
- [6] V. N. Jambhale, P. Amit L., C. Umakant B., Int. J. Sci. Res. Publ., 7(8), 562-565 (2017).
- [7] K. S. Shaaban, E. S. Yousef, E. A. A. Wahab, E. R. Shaaban, S. A. Mahmoud, J. Mater. Eng. Perform., 29(7), 4549-4558 (2020); <https://doi.org/10.1007/s11665-020-04969-6>
- [8] M. R. S. Nasuha, H. Azhan, L. Hasnimulyati, W. A. W. Razali, Y. Norihan, J. Non-Crystalline Solid, 551, 120463 (2021); <https://doi.org/10.1016/j.jnoncrysol.2020.120463>
- [9] S. N. Mohd Rafien, A. Kasim, N. Yahya, A. Hashim, W. A. Wan Razali, Solid State Phenom., 317, 100-108 (2021); <https://doi.org/10.4028/www.scientific.net/SSP.317.100>
- [10] A. F. A. El-Rehim, K. S. Shaaban, J. Mater. Sci. Mater. Electron., 32(4), 4651-4671 (2021); <https://doi.org/10.1007/s10854-020-05204-7>
- [11] P. Goyal, Y. K. Sharma, S. Pal, U. C. Bind, S. C. Huang, S. L. Chung, J. Lumin., 192, 1227-1234 (2017); <https://doi.org/10.1016/j.jlumin.2017.08.061>
- [12] K. Azman, H. Azhan, S. Y. S. Syamsyir, A. Mardhiah, M. R. S. Nasuha, Optical properties of Nd doped lead borotellurite glass, 846, 193-198 (2016); <https://doi.org/10.4028/www.scientific.net/MSF.846.193>
- [13] Y. B. Saddeek, K. Aly, G. Abbady, N. A. K. H. S. Shaaban, A. Dahshan, J. Non-Crystalline Solid, 454, (2016); <https://doi.org/10.1016/j.jnoncrysol.2016.10.023>
- [14] P. Ramesh, G. Jagannath, B. Eraiah, M. K. Kokila, Mater. Sci. Eng., 310, 1-8 (2017); <https://doi.org/10.1088/1757-899X/310/1/012032>
- [15] P. P. Sukul, M. K. Mahata, K. Kumar, J. Lumin., 185, 92-98 (2017); <https://doi.org/10.1016/j.jlumin.2017.01.008>
- [16] D. A. I. Nengli, W. Yanshan, X. U. Bing, Y. Lüyun, Effect of yttrium oxide addition on

absorption and emission properties of bismuth-doped silicate glasses, 30(5). 418-421 (2012);  
[https://doi.org/10.1016/S1002-0721\(12\)60064-7](https://doi.org/10.1016/S1002-0721(12)60064-7)